Songklanakarin J. Sci. Technol.
46 (6), 507–514, Nov. – Dec. 2024

http://www.sjst.psu.ac.th

Original Article

Chitosan nanoparticles from three-spot swimming crab shells for cupric ion adsorption from synthetic wastewater

Metta Kengchuwong[1], Chatyapha Ketwong[2*], Somsuk Trisupakitti[2], Pornpimol Ponkham[2], Panuwat Ketwong[3], and John Morris[4]

[1] *Department of Environmental Science, Faculty of Science and Technology, Rajabhat Maha Sarakham University, Mueang, Mahasarakham, 44000 Thailand*

[2] *Department of Chemistry, Faculty of Science and Technology, Rajabhat Maha Sarakham University, Mueang, Mahasarakham, 44000 Thailand*

[3] *Department of Information Innovation and Water Resources Engineering, Faculty of Science and Technology, Rajabhat Maha Sarakham University, Mueang, Mahasarakham, 44000 Thailand*

[4] *School of Industrial Education and Technology, King Mongkut's Institute of Technology Ladkrabang, Lat Krabang, Bangkok, 10520 Thailand*

Received: 2 May 2024; Revised: 1 August 2024; Accepted: 23 September 2024

Abstract

Chitosan (CT) and chitosan nanoparticles (CTNP), extracted from three-spot swimming crab (*Portunus sanguinolentus*) shells by deacetylation and then ionic gelation, were used to removed pollutants from wastewater. Chitin deacetylation yield to form chitosan was ~75%, measured from FT-IR spectral peak area. After forming CTNP, the FT-IR spectra showed overlapped peaks for COO^- of gum arabic, used for gelation, and NH_3^+ at 1,417 cm^{-1} and the amino group at 1,554 cm^{-1} of chitosan. Adsorption and kinetics for Cu^{2+} removal by both CT and CTNP were compared. CTNP adsorption matched a Langmuir isotherm. Cu^{2+} adsorption by CTNP followed a second-order reaction, indicating bonding of Cu^{2+} to the nanoparticles. CTNP was much more effective and faster in adsorbing Cu^{2+} than CT by 52%, after only a 5-minute reaction time. When using CTNP, the optimum loading was 0.5 g/100 L, at pH 5, 300 rpm and 30 min.

Keywords: chitosan, chitosan nanoparticles, cupric ions, three-spot swimming crab shells

1. Introduction

Chitosan is a natural polymer; it is a derivative of chitin, that can be extracted from shrimp shells, crabs, squid, insect shells, seashells and cell walls of some mushrooms, fungi or algae (Adekanmi, Adekanmi, Adekanmi, Ahmad, & Emmanuel, 2023; Eulalio, Rodrigues, Kleilton, Peniche, & Marcus, 2019; Ghormade, Pathan, & Deshpande, 2017; Kou, Peters, & Mucalo, 2021). By removing the chitin acetyl group in a deacetylation reaction, the N-acetyl glucosamine structure of chitin becomes glucosamine. The chitosan powder thus formed is soluble in weak acids, including acetic, propionic, lactic, pyruvic, malic, tartaric and citric acids (Roy *et al.*, 2017) as well as in strong acids, e.g. nitric or hydrochloric and slightly soluble in phosphoric acid (0.09 M), but insoluble in sulfuric acid (Ardean *et al.*, 2021; Choi, Nam, & Nah, 2016; Roy *et al.*, 2017).

A key property of chitosan-chitin polymers, i.e. natural chitin from which some acetyl groups have been removed, is the degree of acetyl group removal, which affects the properties and function of the polymers (Khor, & Lim,

*Corresponding author
Email address: chatyapha.ke@rmu.ac.th

2003). For example, the molecular weight (determined by the length of the chitosan chain) affects its viscosity**:** high molecular weight chitosan, with longer chains, is more viscous (Zargar, Asghari, & Dashti, 2015). Therefore, chitosan use must consider both the fraction of deacetylation and the molecular weight. Figure 1 shows the structures of chitin and chitosan.

Chitosan contains three reactive functional groups**:** an amino (-NH_2) at C-2, primary alcohol (-CH_2-OH) at C-6, and secondary alcohol groups (-CHOH) at C-3 (Aranaz *et al.*, 2021). Altering these groups produces materials for different applications, e.g. chitosan acts as a flocculant and coagulant, encouraging suspended solids to coagulate and precipitate (Renault, Sancey, Badot, & Crini, 2009). Chitosan performs these functions well because its amino groups can dissociate to provide more positive charge (Renault *et al.*, 2009), causing negative groups in proteins, dyes, free fatty acids and cholesterol to attach to the chitosan positive charges. Also positively charged heavy metal ions bind to the negatively charged chitosan amino group forming complexes (Piekarska *et al.*, 2023). Further, the chitosan amino group form ligands to heavy metals in water better than the chitin acetyl group (Maruca, Suder, & Wightman, 1982).

The large surface area relative to their size allows 10 to 1,000 nm nanoparticle dispersions to efficiently absorb pollutants (Divya, & Jisha, 2018). They can be readily prepared, e.g. by solvent evaporation, emulsion polymerization, or interfacial polymerization (Nagavarma *et al.*, 2012). However, these techniques are complicated and involve harsh conditions, e.g. organic solvents, heat, radiation, or high shear forces (Kumar, Dilbaghi, Saharan, & Bhanjana, 2012).

Complex coacervation or ionic gelation is a non-aggressive method to synthesize nanoparticles, using a simple, uncomplicated method, i.e. stirring at room temperature. Generally, a water-soluble polymer with an oppositely charged polymer is used in a process that is easily upgraded from laboratory to industrial scale (Hoang *et al.*, 2022; Gadziński *et al.*, 2023). Nanoparticles prepared by ionic gelation use oppositely charged polymers, that is, positively (e.g. chitosan) and negatively (e.g. acacia or sodium carboxymethycellulose) charged ones. However, chitosan alone can use intramolecular and intermolecular cross links to form nanoparticles (Abreu *et al.*, 2018; Wang *et al.*, 2022).

Currently, heavy metals in the environment are a major problem; they accumulate through food chains in the ecosystem and affect all living organisms, including humans. One problematic metal is copper (Abreu *et al.*, 2018)**:** it has a high density, boiling and melting points, and is found naturally in soil, rock, water and air, as the free metal or in many Cu compounds (Islam *et al.*, 2013). In excess, it becomes toxic, causing nausea and vomiting or inflammations. Therefore, it is necessary to remove copper from wastewater before releasing it into natural water sources. Many techniques - chemical sedimentation, adsorption, membrane separation, and ion exchange processes, etc. – have been studied. Here we show the effectiveness of nano-chitosan, prepared from crab shells, from which chitosan nanoparticles were formed, together with gum arabic and using sodium pyrophosphate as a crosslinker.

The three-spot swimming crab (*Portunus sanguinolentus*) is extensively harvested in estuaries of the Indian and Western Pacific Oceans, but the shells are waste and thus any use of them is beneficial as reduction of waste. Thus, use of these shells to absorb copper from waste water may add value to the shells without leading to toxic side effects.

The key contribution of this paper is the efficient and cost effective production and use of nanoparticles to reduce heavy metal pollution in waste water. Additionally, we show that these nanoparticles can be formed from readily available sources, that have not been hitherto exploited, and that might otherwise be waste and incur further costs to manage them.

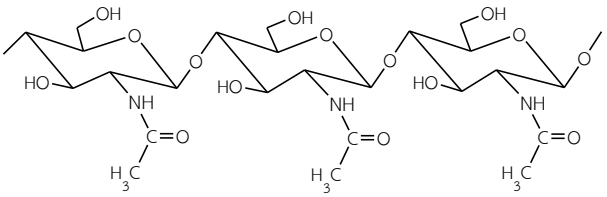

(a) Chitin

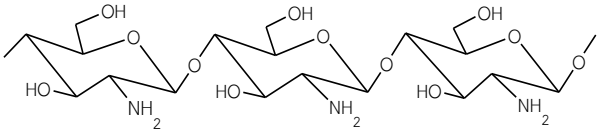

(b) Chitosan

Figure 1. Structures of (a) chitin; and (b) chitosan (Zargar, Asghari, & Dashti, 2015)

2. Materials and Methods

Materials used included hydrochloric acid, sodium hydroxide, methanol, acetone, acetic acid, copper sulfate ($CuSO_4.5H_2O$) and ammonium hydroxide (all AR grade from Carlo Erba); sodium pyrophosphate, $Na_4P_2O_7$ (AR grade from Acros Organics) and Gum Arabic (AR grade from SD Fine Chemicals, Mumbai). These AR grade chemicals were used without further processing.

2.1 Chitin extraction and chitosan preparation from crab shells

Shells were removed from the crabs, washed thoroughly, separated from the flesh, washed again and heated (100 °C, 4 h). Then they were ground and sifted through a 1 mm sieve.

2.1.1 Extraction of chitin from crab shells

Firstly, limestone was removed from the shell, by soaking in 1 M hydrochloric acid at a ratio of 1:10 shell:acid (w/v) at room temperature for 1 hour, followed by discarding the acid and repeating until no more bubbles formed. Typically five cycles sufficed and then they were rinsed until the pH was neutral. Protein was eliminated by boiling in 1 M NaOH at a ratio of 1:20 (w/v) at 90 °C for 2 hours. Samples were washed and pigments removed, by immersion in methanol at a ratio of 1:10 (w/v) shells:methanol for 1 hour, and then the methanol was discarded, followed by immersion in acetone at a ratio of 1:10 (w/v) shells:acetone, for 1 h, and

finally rinsed and dried (70 °C, 18 h) to obtain chitin. The chitin yield was typically 63% of the shell dry mass.

2.1.2 Chitosan preparation

To form chitosan, the prepared chitin was boiled (12.5 M NaOH, 100 °C, 1:20 (w/v) chitin:NaOH, 2 h) allowed to cool and washed until the pH was neutral. The samples were dried at 70 °C for 18 hours to obtain chitosan. Chitosan yield was typically 85% (dry basis).

2.2 Degree of acetyl group degradation

Acetyl group removal from chitosan powder (deacetylation) was measured from a Fourier Transform Infrared (FTIR) spectrum. The ratio between the areas under the peaks of C=O and O-H function group vibrations were converted from % transmission to absorbance and used to calculate the degree of deacetylation (%DD) (Czechowska-Biskup, *et al.*, 2012):

$$\%DD = \frac{[(A_{1655}/A_{3450})] \times 100}{1.33} \quad (1)$$

where A_{1655} is the absorbance of the C=O group at 1,655 cm^{-1}, and A_{3450} is the absorbance of the O-H group at 3,450 cm^{-1}.

2.3 Preparation of chitosan nanoparticles

2.3.1 Preparation of chitosan solution

2 g chitosan powder was dissolved in 100 mL 0.35 M acetic acid and stirred until the chitosan powder dissolved completely. The chitosan solution was viscous and light yellow. This solution was diluted with distilled water to obtain 0.2% w/v chitosan solution.

2.3.2 Preparation of 30 mM sodium pyrophosphate solution

13 g sodium pyrophosphate ($Na_4P_2O_7 \bullet 10H_2O$) was dissolved in 1 L deionized water. The solution was clear and colorless.

2.3.3 Preparation of 0.3%w/v gum arabic solution

2 g Gum Arabic (GA) powder was dissolve in 100 mL deionized water and stirred until the powder dissolved completely. The solution was viscous and pale yellow. This solution was then diluted with distilled water to obtain 0.3% w/v GA solution.

2.3.4 Generation of chitosan nanoparticles using ionic gelation method

To 200 mL 0.2%w/v chitosan in acetic acid, 152 mL 30 mM sodium pyrophosphate solution was added, while stirring at 600 rpm, to form an opaque colloid. After that, 0.3% w/v GA solution was added and rested for 10 min. The suspension was centrifuged to separate the chitosan nanoparticles (4,000 rpm, 15 min). The particles were washed three times with distilled water. After that, chitosan nanoparticles were loaded into a vial and refrigerated for 24 h. Nanochitosan was obtained in cold distilled water, and the nanoparticles were dried in a freezer (-54 °C, 18 h). The dried chitosan nanoparticles were stored in the dark at room temperature (Gadziński *et al.*, 2023).

2.4 Preparation of cupric ion reference solution

The maximum absorption wavelength of $CuSO_4$ in water was at 638 nm. Cupric ion reference solutions were prepared at $CuSO_4.5H_2O$ concentrations from 100 to 350 mg/L. Absorbances were measured at 638 nm to create a calibration curve:

Absorbance = $0.0005[Cu^{2+}] + 0.0023$, $R^2 = 0.99$, for determining $[Cu^{2+}]$ in the synthetic wastewater.

2.5 Factors affecting the adsorption efficiency

To find the optimum adsorption conditions for Cu^{2+} in the synthetic water samples, Cu^{2+} reference solutions were prepared from $CuSO_4 \bullet 5H_2O$ (150 ppm) and amounts of chitosan and the adsorption times were measured.

2.5.1 Influence of sorbent quantity

Chitosan nanoparticles (0.05, 0.1 and 0.5 g) were weighed into a 250 mL beaker, 100 mL copper reference solution (150 ppm) was added and stirred at pH 5 for 60 min. pH was checked with a pH meter. A 9 mL sample of the solution was drawn through a 0.45 µ filter attached to a syringe. The solution was placed in a test tube and 3 mL 0.34 M NH_4OH added and let stand for 15 min. The absorbance was measured at 638 nm and converted to Cu^{2+} content using the calibration curve to calculate Cu^{2+} remaining in the synthetic sample.

2.5.2 Influence of adsorption time

To determine the chitosan nanoparticle absorption dynamics, we took 100 mL 150 ppm Cu^{2+} reference solution, to which varying numbers of chitosan nanoparticles were added. At pH 5, each flask was stirred for 5 to 80 min. 9 mL of the solution was dropped into a test tube, 3 mL 0.34 M NH_4OH was added and it was let stand for 15 min. The absorbance of the solution was measured at 638 nm and compared with the calibration curve to calculate the remaining Cu^{2+} content in the sample.

2.6 Cupric ion adsorption behavior

To determine cupric ion adsorption capacity, 0.5 g chitosan nanoparticles were added to 100 mL cupric ion solutions, with $CuSO_4.5H_2O$ concentrations from 250 to 350 ppm, and stirred at 300 rpm with a magnetic stirrer at pH 5 for 30 min. The remaining Cu^{2+} ion content was analyzed by optical absorption at 638 nm. Then, the concentrations were normalized to plot either Langmuir or Freundlich isotherms.

The Langmuir adsorption equation can be written as (Sarvestani, Esmaeili, & Ramavandi, 2016):

$$\frac{1}{q_e} = \frac{1}{bK_LC_e} + \frac{1}{K_L} \quad (2)$$

where q_e is the amount of sorbent (mg) to the amount of sorbent (g) at equilibrium, *b* is the maximum amount absorbed (mg/g) absorbed, K_L is the energy constant of adsorption or Langmuir's constant (L/mg) and C_e is the equilibrium sorbent concentration (mg/L).

The Freundlich adsorption equation can be written as (Foroutan *et al.*, 2019):

$$\log q_e = \log k_f + ½ \log C_e \quad (3)$$

where C_e is the equilibrium sorbent concentration (mg/L), q_e is the amount of sorbent (mg) to the amount of sorbent (g) at equilibrium, k_F is the multilayer adsorption capacity constant (mg/L), and *n* is a constant related to the energy of adsorption.

Commonly used equations describing the adsorption kinetics between the sorbent solution and sorbent solid phase follow pseudo-first order and pseudo-second order kinetics (Sarvestani, Esmaeili, & Ramavandi, 2016; Foroutan *et al.*, 2019).

Pseudo-first order

$$\log (q_e - q_t) = \log q_e - k_1 t \quad (4)$$

Pseudo-second order

$$\frac{t}{q_t} = \frac{1}{k_2 q_e^2} + \frac{t}{q_e} \quad (5)$$

where k_1 is the first-order reaction rate constant (min), k_2 is the rate constant of the second order reaction (L/mg), t is the adsorption time (min), q_t is the adsorption capacity at time, t (mg/g) and q_e is the amount of sorbent (mg) to the amount of sorbent (g) at equilibrium.

2.7 Cupric ion adsorption efficiency - chitosan *versus* chitosan nanoparticles

0.5 g chitosan powder or chitosan nanoparticles were weighed into a set of 250 mL beakers and 100 mL of 150 ppm copper reference solution was added and stirred at pH 5. The beakers were stirred for 5, 10, 20, 30, 50 or 60 min. 9 mL solution was transferred to a test tube, 3 mL 0.34 M NH_4OH was added and left for 15 min. The absorbance was measured at 638 nm and the calibration curve used to calculate the remaining Cu^{2+} content in the sample.

3. Results and Discussion

In brief, we took crab shell samples to extract chitin and prepared chitosan from them. The degree of deacetylation (%DD) of the prepared chitosan (CT) was analyzed. This chitosan was then used to generate chitosan nanoparticles (CTNP) using ionic crosslinking or ionic gelation techniques. CT or CTNP were then used to adsorb Cu^{2+} in the synthetic wastewater and adsorption capacity was measured optically. Details follow in the next section.

3.1 Chitosan and chitosan nanoparticles

The constituents of the crab shells are minerals (16.8%), proteins (18.3%), pigments (1.8%) and chitin extracted from the shells (63.0%). The yield of chitosan produced from the crab shells was 85%.

The CT prepared from crab shells was analyzed by FTIR spectroscopy - see spectra in Figure 2. Peaks for O-H stretching (3,600-3,200 cm^{-1}), C-H stretching (2,921-2,877 cm^{-1}), C=O stretching of amide (1,645 cm^{-1}) and N-H (amide II) (1,573 cm^{-1}) were observed.

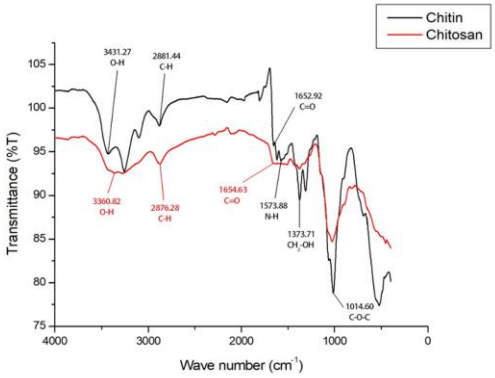

(a) Chitin and chitosan prepared from crab shells

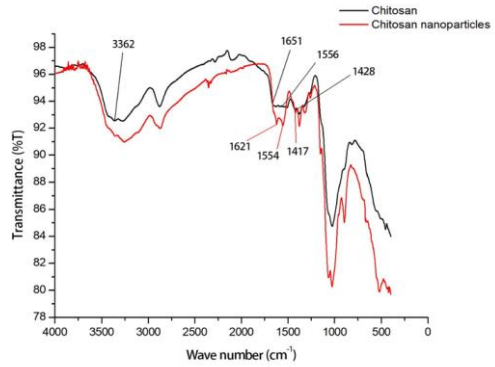

(b) Chitosan and chitosan nanoparticles

Figure 2. FTIR spectra: Chitin, chitosan (CT) and chitosan nanoparticles (CTNP)

The acetyl group removal in chitosan, %DD, computed from FTIR spectral peak areas, was 75%. FTIR analysis of the of chitosan nanoparticles (CTNP) showed the spectrum in Figure 2(b). When chitosan (CT) was analyzed by FTIR, acetyl-glucosamine vibrations at 1,428 and 3,362 cm^{-1}, and amine and amide II bending vibrations at 1,651 and 1,556 cm^{-1} were found. The acetyl-glucosamine at 1,351 cm^{-1} and carboxyl COO^- bond stretching at 1,621 cm^{-1} were derived from crosslinking of gum arabic (GA), confirming that crosslinking occurred. Overlaps between the GA COO^- group and the chitosan NH_3^+ group at 1,417 cm^{-1} and the amino group at 1,554 cm^{-1} were observed. Scanning Electron Microscopy (SEM) images of the chitosan nanoparticles, taken before absorbing copper ions, are shown in Figure 3.

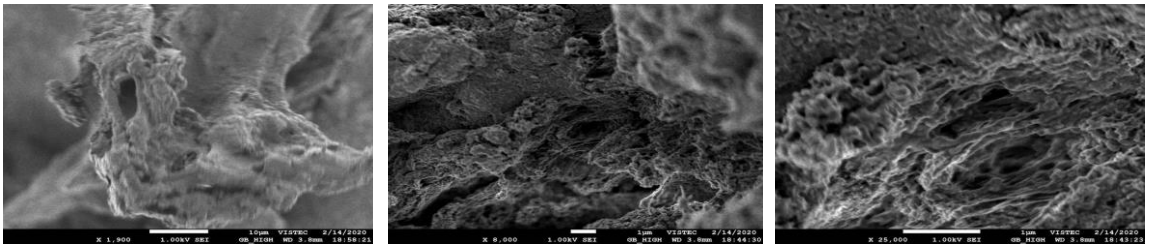

(a) (b) (c)

Figure 3. SEM images of chitosan nanoparticles (CTNP) before copper ion adsorption at (a) 1,900×, (b) 8,000× and (c) 25,000× magnification

3.2 Cupric ion adsorption efficiency

In this section, the optimum factors for Cu^{2+} adsorption in our synthetic wastewater using chitosan nanoparticles (CTNP) as adsorbent were studied including amount of chitosan (CT) and adsorption time.

3.2.1 Influence of sorbent content

To measure the influence of sorbent content, 0.05, 0.1 and 0.5 g CTNP were added to the reference 150 ppm Cu^{2+} solution and stirred at pH 5 and 300 rpm for 60 min. Samples were taken and analyzed at the times shown in Figure 4.

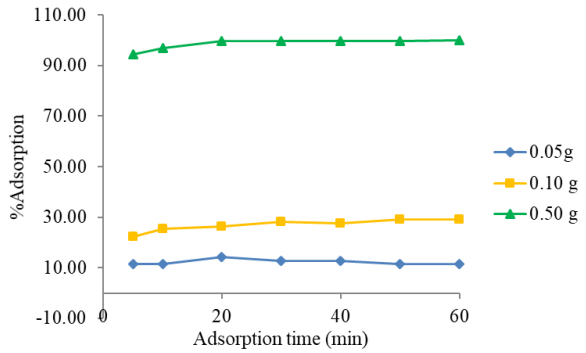

Figure 4. Adsorption of Cu^{2+} with various CTNP loadings

As expected, Figure 4 shows that increased adsorbent loading resulted in higher Cu^{2+} absorption fractions because the adsorbent surface area was larger.

3.2.2 Influence of adsorption time

Adsorption times from 5 to 80 min were measured, using 0.5 g CTNP, which was able to adsorb most of the Cu^{2+}. The adsorption fractions from Cu^{2+} solutions, at concentrations of 250, 300 and 350 ppm, stirred at 300 rpm over up to 80 min, are shown in Figure 5.

From Figure 5, copper absorption increased rapidly up to about 30 min and leveled off after that, consistent with the adsorption experiments using chitosan powder. It was found that during 5 − 30 min copper ions diffuse into the pores of adsorbent. It was found that the slope of the graph increased. But when the adsorption time was increased to 60 − 80 min, the percentage of adsorption tended to change to unstable due to ion elution occurring or adsorption to equilibrium.

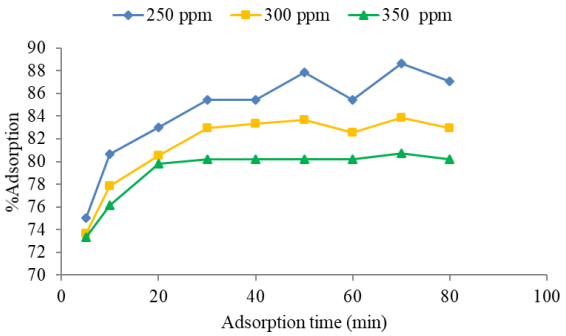

Figure 5. Adsorption by CTNP - fraction of Cu^{2+} ions in wastewater samples

3.3 Cupric ion adsorption behavior

The Cu^{2+} adsorption model was determined, using a loading of 0.5 g CTNP in 100 mL, and concentrations ranging from 250 to 350 ppm, under stirring at 300 rpm at pH 5 for 30 min. The remaining Cu^{2+} adsorption was analyzed – see Langmuir or Freundlich models in Figure 6.

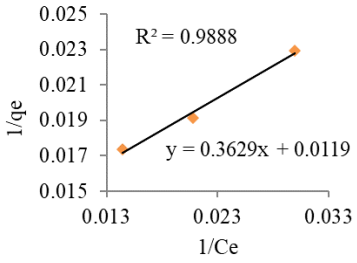

Langmuir isotherm

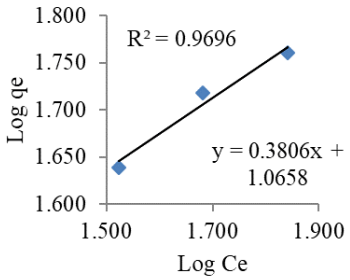

Freundlich isotherm

Figure 6. Adsorption isotherms of Cu^{2+} adsorption with 0.5 g CTNP at pH 5

Adsorption isotherm parameters derived from linear equation fits using the Langmuir model were $K = 3.28 \times 10^{-2}$ and $q_m = 84.03$ ($R^2 = 0.9888$) and using the Freundlich model gave $k = 1.066$ and $n = 2.63$ ($R^2 = 0.9696$). The correlation coefficient, R^2, showed that Cu^{2+} adsorption with CTNP was consistent with Langmuir model. This indicated that chitosan nanoparticles adsorbed a monolayer of Cu^{2+} ions.

For determining kinetics of Cu^{2+} adsorption by CTNP, Cu^{2+} concentrations from 250 – 350 ppm and 0.5 g/100 mL CTNP loadings were used (Figure 7).

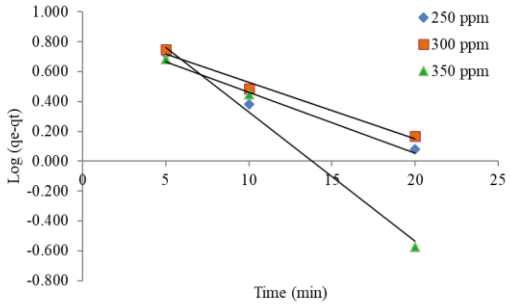

(a) pseudo-first order

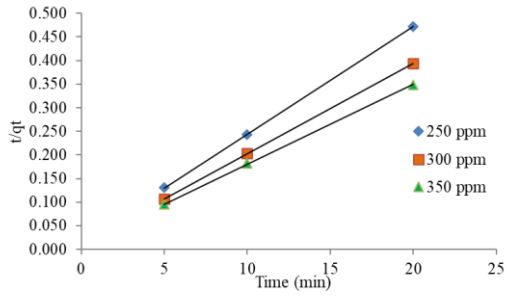

(b) pseudo-second order

Figure 7. Cu^{2+} adsorption fitted using (a) pseudo-first, and (b) pseudo-second order kinetics

Figure 7 shows plots of data points derived from assuming pseudo-first (a) or pseudo-second (b) order reactions. The correlation coefficient (R^2) indicated a second-order reaction, consistent with Abreu *et al.* (2018). Thus, Cu^{2+} was absorbed on chitosan nanoparticles using chemical forces resulting from sharing of electrons of Cu^{2+} ions with -OH and $-NH_2$ functional groups in the nanoparticles. Cu^{2+} is a metal group that has properties on borderline between the strong and weak acids and thus can form coordination bonds with both hard and soft ligands (including -OH and $-NH_2$), within the chitosan chain (Lone, Yoon, Lee, & Cheong, 2019).

3.4 Adsorption efficiency

We compared the Cu^{2+} adsorption efficiency for chitosan (CT) and chitosan nanoparticles (CTNP). 0.5 g CT or CTNP was loaded to 100 mL of our reference 150 ppm Cu^{2+} solution and absorption monitored for 50 min: residual Cu^{2+} concentrations are shown in Figure 8.

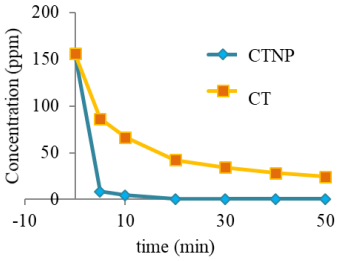

Figure 8. Remaining Cu^{2+} concentration after adsorption by CT and CTNP

Figure 8 shows that, after 5 minutes, the amount of Cu^{2+} remaining after adsorption with CTNP was considerably less than that remaining with CT. The CNTP polymer chain had hydroxyl (-OH) and amino ($-NH_2$) groups that were cross-linked with sodium pyrophosphate making the base CT chain longer: further, gum arabic added a carboxyl group (COO^-), that can bind to heavy metals. Thus, the nanoparticles (CTNP) were much more effective at adsorbing Cu^{2+} than chitosan alone (Lone, Yoon, Lee, & Cheong, 2019).

When the nanoparticles after Cu^{2+} adsorption were examined by SEM, CTNP had a smoother surface than the CT images, indicating that metal ions attached to the CTNP – see Figure 9.

4. Conclusions

Chitin was simply extracted from waste crab shells by demineralization with hydrochloric acid and protein removal with sodium hydroxide. Chitosan was then extracted from chitin by removing the acetyl groups in concentrated sodium hydroxide, at ratio of 50% mass per volume. The chitosan yield was 85%. The extracted chitosan was synthesized into chitosan nanoparticles by ionic gelation with gum arabic and sodium pyrophosphate as crosslinking agents. SEM images showed rough surfaces with many pores.

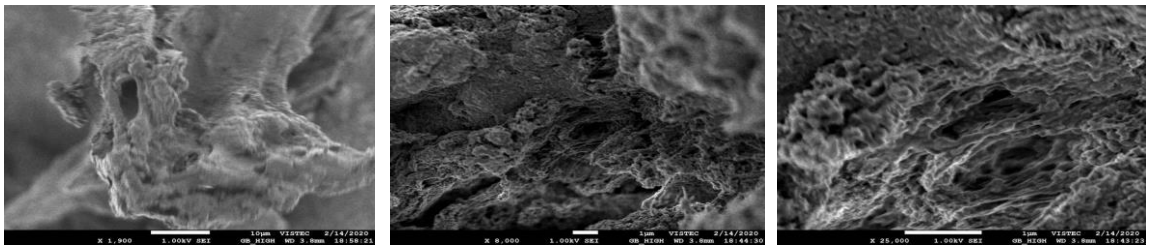

(a) (b) (c)

Figure 9. SEM images of CTNP after metal ion adsorption at (a) 1,000×, (b) 1,900× and (c) 19,000× magnification

This project showed that one readily available, high volume waste – crab shells - could be transformed by simple, inexpensive steps into an absorbent that, rather than presenting a further challenge as waste in the environment, could be used to remove another troublesome and toxic pollutant – copper - from water sources. Further, although the chitosan alone was effective in removing a heavy metal, its removal efficiency was improved by several factors on transforming it into nanoparticles by a further simple and inexpensive process.

Although this project focused on waste that is plentiful in our region, other chitin sources, e.g. prawn shells (16-40% chitin) (Zhao *et al.*, 2019), fish scales (20-30% chitin) (Sumathi, Vignesh, & Madhusudhanan, 2017) and other marine products (Coppola *et al.*, 2021) are expected to be similarly effective. Chitin has also been used to remove other toxic metals (Maruca, Suder, & Wightman, 1982; Foroutan *et al.*, 2019) and the nanoparticles described here would be expected to enhance removal of many similar pollutants.

Acknowledgements

We thank the laboratory staff of the Science Center of Rajabhat Maha Sarakham University for allowing us to use their facilities and instruments, which allowed this project to succeed, and Vidyasirimedhi Institute of Science and Technology (VISTEC) for assistance with the FT-IR spectra and SEM images.

References

Abreu, F. O. M. D. S., Silva, N. A. D., Sipauba, M. D. S., Pires, T. F. M., Bomfim, T. A., Monteiro Junior, O. A. D. C., & Forte, M. M. D. C. (2018). Chitosan and gum arabic nanoparticles for heavy metal adsorption. *Polímeros, 28*, 231-238. doi:10.1590/0104-1428.02317

Adekanmi, A. A., Adekanmi, U. T., Adekanmi, A. S., Ahmad, L. K., & Emmanuel, O. O. (2023). Production and characterisation of chitosan from chitin of snail shells by sequential modification process. *African Journal of Biotechnology, 22*(2), 39-53. doi:10.5897/AJB2020.17135

Aranaz, I., Alcántara, A. R., Civera, M. C., Arias, C., Elorza, B., Heras Caballero, A., & Acosta, N. (2021). Chitosan: An overview of its properties and applications. *Polymers, 13*(19), 3256. doi:10.3390/polym13193256

Ardean, C., Davidescu, C. M., Nemes, N. S., Negrea, A., Ciopec, M., Duteanu, N., . . . Musta, V. (2021). Factors influencing the antibacterial activity of chitosan and chitosan modified by functionalization. *International Journal of Molecular Sciences, 22*(14), 7449. doi:10.3390/ijms22147449

Choi, C., Nam, J. P., & Nah, J. W. (2016). Application of chitosan and chitosan derivatives as biomaterials. *Journal of Industrial and Engineering Chemistry, 33*, 1-10. doi:10.1016/j.jiec.2015.10.028

Coppola, D., Lauritano, C., Palma Esposito, F., Riccio, G., Rizzo, C., & de Pascale, D. (2021). Fish Waste: from Problem to Valuable Resource. *Marine Drugs, 19*, 116. doi:10.3390/md19020116

Czechowska-Biskup, R., Jarosinska, D., Rokita, B., Ulanski, P., & Rosiak, J. M. (2012). Determination of degree of deacetylation of chitosan comparision of methods. Progress on Chemistry and Application of chitin and its, Volume XVII, 5-20. Retrieved from https://www.researchgate.net/publication/288104933_Determination_of_degree_of_deacetylation_of_chitosan_-_Comparision_of_methods

Divya, K., & Jisha, M. S. (2018). Chitosan nanoparticles preparation and applications. *Environmental Chemistry Letters, 16*, 101-112. doi:10.1007/s10311-017-0670-y

Eulalio, H. Y. C., Rodrigues, J. F. B., Kleilton, O., Peniche, C., & Marcus, V. (2019). Characterization and thermal properties of chitosan films prepared with different acid solvents. *Revista Cubana de Química, 31*(3), 309-323. Retrieved from https://www.redalyc.org/journal/4435/443561090001/html/

Gadzinski, P., Froelich, A., Jadach, B., Wojtylko, M., Tatarek, A., Bialek, A., Krysztofiak, J., . . . Osmalek, T. (2023). Ionotropic gelation and chemical crosslinking as methods for fabrication of modified-release gellan gum-based drug delivery systems. *Pharmaceutics, 15*(1), 108. doi:10.3390/pharmaceutics15010108

Ghormade, V., Pathan, E. K., & Deshpande, M. V. (2017). Can fungi compete with marine sources for chitosan production. *International Journal of Biological Macromolecules, 104*, 1415-1421. doi:10.1016/j.ijbiomac.2017.01.112

Foroutan, R., Mohammadi, R., Farjadfard, S., Esmaeili, H., Ramavandi, B., & Sorial, G.A. (2019). Eggshell nano-particle potential formethyl violet and mercury ion removal: Surface study and field application. *Advanced Powder Technology, 30*(10), 2188-2199. doi:10.1016/j.apt.2019.06.034

Hoang, N. H., Le Thanh, T., Sangpueak, R., Treekoon, J., Saengchan, C., Thepbandit, W., . . . Buensanteai, N. (2022). Chitosan nanoparticles-based ionic gelation method: A promising candidate for plant disease management. *Polymers, 14*(4), 662. doi:10.3390/polym14040662

Islam, F., Bhattacharjee, S. C., Hossain, A., Islam, S., Mahmud, A. S. M., Ahmed, Y., & Rahman, M. (2013). Assessment of copper in diverse pulses, bananas, vegetables and arums of five upazila of Chittagong area in Bangladesh by spectrophotometric method. *International Food Research Journal, 20*(4), 1867-1871.

Khor, E., & Lim, L. Y. (2003). Implantable applications of chitin and chitosan. *Biomaterials, 24*(13), 2339-2349. doi:10.1016/S0142-9612(03)00026-7

Kou, S. G., Peters, L. M., & Mucalo, M. R. (2021). Chitosan: A review of sources and preparation methods. *International Journal of Biological Macro molecules, 169*, 85-94. doi:10.1016/j.ijbiomac.2020.12.005

Kumar, S., Dilbaghi, N., Saharan, R., & Bhanjana, G. (2012). Nanotechnology as emerging tool for enhancing

solubility of poorly water-soluble drugs. *Bionano science, 2*, 227-250. doi:10.1007/s12668-012-0060-7

Lone, S., Yoon, D. H., Lee, H., & Cheong, I. W. (2019). Gelatin-chitosan hydrogel particles for efficient removal of Hg(II) from wastewater. *Environmental Science: Water Research and Technology, 5*(1), 83-90. doi:10.1039/C8EW00678D

Maruca, R., Suder, B. J., & Wightman, J. P. (1982). Interaction of heavy metals with chitin and chitosan. III. Chromium. *Journal of Applied Polymer Science, 27*(12), 4827-4837. doi:10.1002/app.1982.070271227

Nagavarma, B. V. N., Yadav, H. K., Ayaz, A. V. L. S., Vasudha, L. S., & Shivakumar, H. G. (2012). Different techniques for preparation of polymeric nanoparticles-a review. *Asian Journal of Pharma ceutical and Clinical Research, 5*(3), 16-23. Retrieved from https://www.researchgate.net/publication/279545193_Different_techniques_for_preparation_of_polymeric_nanoparticles-_A_review

Piekarska, K., Sikora, M., Owczarek, M., Jóźwik-Pruska, J., & Wiśniewska-Wrona, M. (2023). Chitin and chitosan as polymers of the future - Obtaining, modification, life cycle assessment and main directions of application. *Polymers, 15*(4), 793. doi:10.3390/polym15040793

Renault, F., Sancey, B., Badot, P. M., & Crini, G. (2009). Chitosan for coagulation/flocculation processes–an eco-friendly approach. *European Polymer Journal, 45*(5), 1337-1348. doi:10.1016/j.eurpolymj.2008.12.027

Roy, J. C., Salaün, F., Giraud, S., Ferri, A., Chen, G., & Guan, J. (2017). Solubility of chitin: solvents, solution behaviors and their related mechanisms. *Solubility of Polysaccharides, 3*, 20-60. doi:10.5772/intechopen.71385

Sarvestani, F.S., Esmaeili, H., & Ramavandi, B. (2016). Modification of Sargassum angustifolium by molybdate during a facile cultivation for high-rate phosphate removal from wastewater: structural characterization and adsorptive behavior. *Biotechnology, 6*, 251. doi:10.1007/s13205-016-0570-z

Sumathi, N., Vignesh, R., & Madhusudhanan, J. (2017). Extraction, characterization and applications of chitosan from fish scales. *International Journal of Modern Trends in Engineering and Research, 4*(4), 137-141. doi:10.21884/ijmter.2017.4131.q8njr

Wang, W., Meng, Q., Li, Q., Liu, J., Zhou, M., Jin, Z., & Zhao, K. (2020). Chitosan derivatives and their application in biomedicine. *International Journal of Molecular Sciences, 21*(2), 487. doi:10.3390/ijms21020487

Zargar, V., Asghari, M., & Dashti, A. (2015). A review on chitin and chitosan polymers: Structure, chemistry, solubility, derivatives, and applications. *ChemBio Eng Reviews, 2*(3), 204-226. doi:10.1002/cben.201400025

Zhao, D., Huang, W. C., Guo, N., Zhang, S., Xue, C., & Mao, X. (2019). Two-step separation of chitin from shrimp shells using citric acid and deep eutectic solvents with the assistance of microwave. *Polymers (Basel), 11*(3), 409. doi:10.3390/polym11030409